

Two-channel Kondo tunneling in triple quantum dot

T. Kuzmenko¹, K. Kikoin¹ and Y. Avishai^{1,2}

¹Department of Physics and ²Ilse Katz Center, Ben-Gurion University, Beer-Sheva, Israel
(Dated: May 21, 2019)

A triple quantum dot with odd occupation weakly connected in series with metallic electrodes is shown to display a generic two-channel Kondo physics. Renormalization group equations for the exchange constants are written down (to third order) and solved for any initial condition. The structure of the conductance as function of temperature and gate voltage is then analyzed, implying that an experimentally controlled transition between single channel (a Fermi liquid) and two-channel (non-Fermi liquid) behavior is feasible. At even occupation, there is no over-screening and a Fermi liquid behavior is expected.

PACS numbers:

Motivation: In the present work, a simple configuration of localized moment in nanostructures is studied, where the two-channel Kondo effect is responsible for resonance tunneling. Concrete experiment is proposed, whose importance is evident, since a multichannel Kondo system is known to be a non-Fermi liquid [1], but construction of simple theoretical models pertaining to experimentally feasible setups is notoriously elusive. Examples are magnetic impurity scattering, physics of two-level systems and Kondo lattices (see [2, 3] for review). Recent attempts to realize two-channel Kondo effect in tunneling through quantum dots [4] using peculiar setups still await experimental manifestation. The problem is exemplified in tunneling through a simple quantum dot sandwiched between two metallic "left" (l) and "right" (r) leads. Starting from the single impurity Anderson model, it is tempting to think of the two leads as a source of two tunneling channels. However, if the two fermion lead operators $c_{k\sigma a}$ (k = momentum, σ = spin projection and $a = l, r$ the lead index) are coupled to a single dot electron operator d_σ , one channel can always be eliminated by an appropriate rotation in $l - r$ space [5]:

$$\begin{aligned} c_{k\sigma l} &= \cos\theta_k c_{k\sigma 1} + \sin\theta_k c_{k\sigma 2}, \\ c_{k\sigma r} &= -\cos\theta_k c_{k\sigma 2} + \sin\theta_k c_{k\sigma 1}. \end{aligned} \quad (1)$$

As a result, only the standing wave fermions $c_{k\sigma 1}$ contribute to tunneling. It is therefore natural to expect that a generic two-channel Hamiltonian can be realized only when the rotation (1) cannot eliminate the second channel. Such situation may arise, e.g., when, instead of a simple quantum dot one has a nanoobject consisting of several dots so that $c_{k\sigma l}$ and $c_{k\sigma r}$ are coupled to *different* dot electron operators.

Model Hamiltonian: Consider a triple quantum dot (TQD) which consists of three dots l, f, r , connected in series to left and right leads (see Fig. 1). The figure defines also tunneling amplitudes V_a and hopping amplitudes W_a between the side dots and the central one. The source of Kondo screening is a Coulomb blockade in the central dot f , which is supposed to have a smaller radius (and hence a larger capacitive energy) than the two side dots, namely, $Q_f \gg Q_{l,r}$ (cf. [6]). The tunneling Hamiltonian has the form $H_t = \sum_{a=l,r} \sum_{k\sigma} V_a c_{k\sigma a}^\dagger d_{\sigma a} + H.c.$,

and the rotation (1) does not eliminate the second tunneling channel. Note, however, that the large charging energy Q_f suppresses direct tunneling from the left lead to the right one, so that *only co-tunneling mechanism* contributes to the current. To quantify these elementary

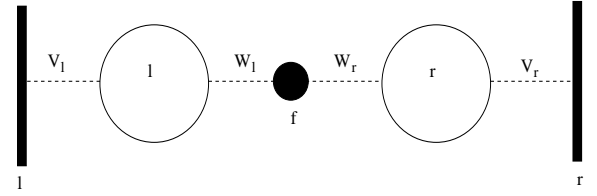


FIG. 1: Triple quantum dot in series.

statements consider the case of TQD with three electrons. The Hamiltonian of the isolated dot reads

$$\begin{aligned} H_d &= \sum_{\alpha=l,r,f} \left(\sum_{\sigma} \varepsilon_{\alpha} n_{\sigma\alpha} + Q_{\alpha} n_{\uparrow\alpha} n_{\downarrow\alpha} \right) \\ &+ \sum_{a=l,r} (W_a d_{\sigma a}^\dagger d_{f\sigma} + H.c.), \end{aligned} \quad (2)$$

where $n_{\sigma a} = d_{\sigma a}^\dagger d_{\sigma a}$, with $\sum_{\sigma a} n_{\sigma a} = 3$. This Hamiltonian can be easily diagonalized in the space of three-electron states $|\Lambda\rangle$ of the TQD. The lowest ones are classified as a ground state doublet $|d_1\rangle$, low-lying doublet excitation $|d_2\rangle$ and quartet excitation $|q\rangle$. The *single electron* levels ε_a ($a = l, r$) are tuned by gate voltages V_{ga} in such a way that $\beta_a \equiv W_a/\Delta_a \ll 1$ ($\Delta_a \equiv \varepsilon_a - \varepsilon_f$). To order β_a^2 , the corresponding energy levels E_Λ are

$$\begin{aligned} E_{d_1} &= \varepsilon_f + \varepsilon_l + \varepsilon_r - \frac{3}{2} \left[\frac{W_l^2}{\Delta_l} + \frac{W_r^2}{\Delta_r} \right], \\ E_{d_2} &= E_{d_1} + \left[\frac{W_l^2}{\Delta_l} + \frac{W_r^2}{\Delta_r} \right], \\ E_q &= \varepsilon_f + \varepsilon_l + \varepsilon_r. \end{aligned} \quad (3)$$

Tunneling into the leads couples three-particle states $|\Lambda\rangle$ of the dot, with two-particle states $|\lambda\rangle$ (four-particle states are excluded since they are much higher in energy). It is then useful to introduce diagonal and number changing dot Hubbard operators $X^{\Lambda\lambda} = |\Lambda\rangle\langle\lambda|$ and

$X^{\lambda\Lambda} = |\lambda\rangle\langle\Lambda|$ respectively. The Hamiltonian of the whole system (leads, TQD and tunneling) then reads

$$H = \sum_{k\sigma a} \epsilon_{ka} c_{k\sigma a}^\dagger c_{k\sigma a} + \sum_{\Lambda} E_{\Lambda} X^{\Lambda\Lambda} + \left(\sum_{\Lambda\lambda} \sum_{k\sigma a} V_{\sigma a}^{\Lambda\lambda} c_{k\sigma a}^\dagger X^{\lambda\Lambda} + H.c. \right). \quad (4)$$

Here $-\frac{D_a}{2} < \epsilon_{ka} < \frac{D_a}{2}$ are lead electron energies with nearly identical bandwidths $D_l \approx D_r \equiv D_1$. Within linear response, the Fermi energies are the same on both sides, $\epsilon_{Fl} = \epsilon_{Fr} = \epsilon_F = 0$. The tunneling amplitudes $V_{\sigma a}^{\Lambda\lambda} \equiv V_a \langle \lambda | d_{\sigma a} | \Lambda \rangle$ depend explicitly on the lead index $a = l, r$ and on the respective 2-3 particle quantum numbers λ, Λ . Elimination of one of the two channels by the rotation (1) is then impossible: adding l or r electron to a given state $|\lambda\rangle$ results in different states $|\Lambda\rangle$.

RG procedure and spin Hamiltonian: Following a two-stage RG procedure the low-energy Kondo tunneling through TQD may be exposed. First, the bandwidth is continuously reduced from D_1 to $D_0 < D_1$ (see [6] and references therein), and the energy levels (3) are renormalized by eliminating high-energy charge excitations [7]. If at the end of this procedure $E_{d_1}(D_0) < -D_0/2$ and $E_{d_2}(D_0) - E_{d_1}(D_0)$ exceeds the Kondo energy T_K (defined below), charge fluctuations are quenched and the doublet ground state $|d_{1\sigma=\uparrow,\downarrow}\rangle$ becomes a localized moment. Following the Schrieffer-Wolff transformation the spin Hamiltonian reads

$$H_s = J_l \mathbf{S} \cdot \mathbf{s}_l + J_r \mathbf{S} \cdot \mathbf{s}_r + J_{lr} \mathbf{S} \cdot (\mathbf{s}_{lr} + \mathbf{s}_{rl}). \quad (5)$$

The spin 1/2 operator \mathbf{S} acts on $|d_{1\sigma=\uparrow,\downarrow}\rangle$ whereas the lead electrons spin operators are $\mathbf{s}_a = \sum_{kk'} c_{k\mu a}^\dagger \boldsymbol{\sigma}_{\mu\nu} c_{k'\nu a}$. The presence of the left-right spin operator $\mathbf{s}_{lr} = \sum_{kk'} c_{k\mu l}^\dagger \boldsymbol{\sigma}_{\mu\nu} c_{k'\nu r}$ is responsible for co-tunneling current. Moreover, $J_a = 8\gamma |V_a|^2 / 3(\epsilon_F - \epsilon_a) > 0$ (where $\gamma = \sqrt{1 - \frac{3}{2}(\beta_l^2 + \beta_r^2)}$), while $J_{lr} = -4V_l V_r \beta_l \beta_r / 3(\epsilon_F - \epsilon_f)$ so that $|J_{lr}/J_a|$ is of order $\beta_l \beta_r \ll 1$. The Hamiltonian (5) then encodes a two-channel Kondo physics, where the leads serve as two independent channels.

In the second stage of the RG procedure, a poor-man scaling technique is used to renormalize the exchange constants by further reducing the bandwidth $D_0 \rightarrow D$. The pertinent fixed points are then identified as $D \rightarrow T_K$ [8]. Unlike the situation encountered in the single-channel Kondo effect, third order diagrams in addition to the usual single-loop ones should be included (see figure 5 in Ref. [1] and figure 9 in Ref. [9]). Below we use D_0 as an energy unit and all energy parameters such as $J_a, V_a, W_a, V_{ga}, \epsilon_a, T, D$ etc. now become dimensionless. The RG equations are,

$$\frac{dJ_a}{d \ln D} = -J_a^2 + J_a(J_l^2 + J_r^2) + J_{lr}^2(J_l + J_r - 1), \quad (6)$$

$$\frac{dJ_{lr}}{d \ln D} = -\frac{J_{lr}}{2} (J_l + J_r) + J_{lr}(J_l^2 + J_r^2). \quad (7)$$

Since $J_{lr}^2/J_a^2 \approx \beta_a^4$ we can safely drop J_{lr}^2 on the RHS of equations (6) and solve them separately starting from an initial condition $J_a(D_0 = 1) = J_{a0}$ (J_{lr} is then obtained by integrating equation (7)). Define $\phi_a \equiv (J_l + J_r - 1)/J_a$, $C_a \equiv \phi_{\bar{a}0} - \phi_{a0}$ and $L_a(x) \equiv x - \ln(1 + C_a/x) - 2 \ln x$ the solution for J_l, J_r is then,

$$L_a(\phi_a) - L_a(\phi_{a0}) = \ln \frac{1}{D} \quad (a = l, r), \quad (8)$$

with $a = l, r$ and $\bar{a} = r, l$. In Ref. [1] equations (6) (disregarding J_{lr}) have been written down *on the symmetry line* $J_l = J_r = J$. Heuristic arguments are then presented leading to a qualitative picture of the flow diagram in the entire quadrant $J_l, J_r > 0$, with a saddle fixed point at $J_l = J_r \equiv J^* = \frac{1}{2}$ and a couple of stable fixed points at $(\infty, 0)$ and $(0, \infty)$. Here the same equations and their solution (8) pertains *apriori* to the entire quadrant and yield figure 2 which is accurate to third order. Higher order corrections may only move J^* away from 1/2. Moreover, even if all the three equations (6,7) are treated simultaneously, the fixed point remains intact.

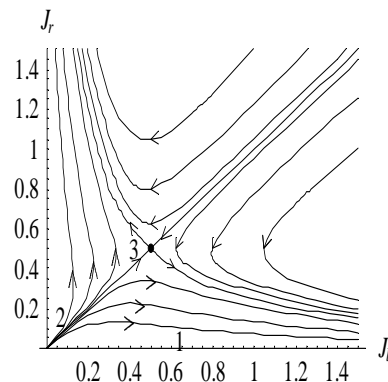


FIG. 2: Scaling trajectories for two-channel model.

Conductance: According to general perturbative expression for the dot conductance [10], its zero-bias anomaly is encoded in the third order term,

$$G^{(3)} = G_0 J_{lr}^2 [J_l(T) + J_r(T)], \quad (G_0 = \frac{2e^2}{h}). \quad (9)$$

Here the temperature T replaces the bandwidth D in the solution (8). Let us present a qualitative discussion of the conductance $G[J_a(T)]$ (or in an experimentalist friendly form, $G(V_{ga}, T)$) based on the flow diagram 2. (Strictly speaking, the RG method and hence the discussion below, is mostly reliable in the weak coupling regime $T > T_K$). Varying T implies moving on either a “non-diagonal” curve $[J_l(T), J_r(T)]$ with, say, $J_l(T) > J_r(T)$, or on the “diagonal” (symmetry) line $[J(T), J(T)]$. On the other hand, varying V_{ga} affects the initial condition (J_{l0}, J_{r0}) enabling motion *perpendicular* to the curves $(J_l(T), J_r(T))$ displayed in figure 2.

1) With lowering T away from the symmetry line, the conductance is enhanced due to Kondo screening near

the left lead, the corresponding Kondo temperature T_K^l is well defined, and $J_l \approx [\ln \frac{T}{T_K^l}]^{-1}$, while $J_r \approx 0$.

2) On the symmetry line at high T , $J_l = J_r \equiv J \ll 1/2$. More precisely, the high T solution (8) yields $J = J_0/(1 + J_0 \ln(T))$, implying a logarithmic growth, similar to the anisotropic case.

3) On the symmetry line as T decreases, the point $[J(T), J(T)]$ climbs and ends at the fixed point $(J^*, J^*) = (1/2, 1/2)$. In its neighborhood equation (8) yields,

$$\frac{1 - 2J}{J} = A(J_0)T^{1/2}, \quad (10)$$

with $A(J_0) = \frac{1-2J_0}{J_0} \exp(1/2J_0)$ independent of T . Thus, $J \rightarrow 1/2$ as $T^{1/2}$ in accordance with an exact solution based on conformal field theory [11].

4) The picture at the entire quadrant $J_l, J_r > 0$ is now unraveled. In a square $0 < J_{l,r} \ll 1/2$, which corresponds to high T , the curves are rather dense and the conductance is virtually constant as one crosses the diagonal. At much lower $T \rightarrow T_K$ we either have $J_a \ll 1/2 \ll J_a$ approaching the Kondo enhanced single channel case, or the less enhanced two channel case $J_l = J_r \rightarrow 1/2$ as in (10). This means that as the diagonal is crossed at low T , there is a dip in the conductance.

To put these results in an experimentally oriented language, consider the conductance $G(V_{ga}, T)$ as function of T for several fixed values of V_{ga} and vice versa, recalling (9). First, holding V_{ga} , one finds that at low $T \rightarrow T_K$ (from above) the value of $G(V_{ga}, T)$ on a non-diagonal curve increases logarithmically with decreasing T while on the diagonal line it saturates according to (10). As T increases much above T_K , $G(V_{ga}, T)$ decreases and saturates logarithmically both on the diagonal and non-diagonal curves, albeit with different paces, since $J_l(T)$ approaches $J(T)$ asymptotically from above (figure 3).

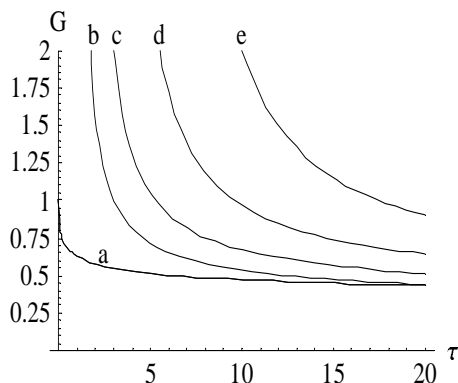


FIG. 3: Conductance G in units of $J_r^2 G_0$ as a function of temperature ($\tau = T/T_K$), at various gate voltages. The lines correspond to: (a) the symmetric case $J_l = J_r$ ($V_g = 0$), (b) $J_l \approx J_r$ ($V_g = 0.002$), (c-e) $J_l \gg J_r$, with $V_g = 0.03, 0.06$ and 0.09 .

Second, holding T and changing J_a (by varying gate voltages V_{ga}) enables an experimentalist to virtually cross the diagonal line and thereby induces a crossover between one

and two-channel situation. Following the discussion preceding figure 3, the conductance $G(V_{ga}, T)$ is anticipated to have a dip at low T which becomes shallower at higher T . This scenario is displayed in figure 4.

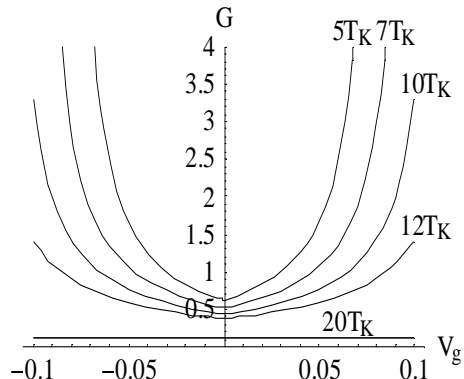


FIG. 4: Conductance G in units of $J_r^2 G_0$ as a function of gate voltage at various temperatures.

Higher degeneracy and dynamical symmetries:

The spin Hamiltonian (5) is expressible in terms of the dot (ground-state) spin $\mathbf{S} = 1/2$ components S_i ($i = x, y, z$), the generators of the group SU_2 . Due to complete spin degeneracy $E_{d_1\uparrow} = E_{d_1\downarrow}$, the dot Hamiltonian itself is of course invariant under SU_2 but the hybridization leading to the exchange terms $J_a \mathbf{S} \cdot \mathbf{s}_a$ clearly breaks it, allowing for dot spin-flips. In composite quantum dots, the degeneracy of spin states at the end of the first stage RG procedure might be much richer[6] (and greater than 2). Our analysis shows that for the present model of TQD with $N = 3$ electrons there exists a scenario of level degeneracy in which the renormalized energies of the two doublets and the quartet are degenerate at the Schrieffer-Wolff limit, that is, $E_{d_1}(D_0) = E_{d_2}(D_0) = E_q(D_0) \leq -D_0/2$. The corresponding wave functions $|\Lambda\rangle$ are vector sums of states composed of a "passive" electron sitting in the central dot and singlet/triplet (S/T) two-electron states in the l, r dots. Using certain combinations of dot Hubbard operators $|\Lambda\rangle\langle\Lambda'|$ one can now define two vector operators \mathbf{S} and \mathbf{M} such that \mathbf{S} is the dot spin 1 operator responsible for transition between different triplet states, while \mathbf{M} accounts for S/T transitions[6]. The operators \mathbf{S} and \mathbf{M} together with the spin operator \mathbf{s} of the central dot electron generate the group $SO_4 \times SU_2$ specified by the Casimir operator $S^2 + M^2 + s^2 = \frac{15}{4}$. The corresponding spin Hamiltonian,

$$H_s = \sum_{a=l,r} [J_a^T \mathbf{S} + J_a^{ST} \mathbf{M}] \cdot \mathbf{s}_a + J_{lr} \mathbf{s} \cdot (\mathbf{s}_{lr} + \mathbf{s}_{rl}) \quad (11)$$

expressible in terms of its generators breaks that symmetry. Here $J_a^T = 4\gamma|V_a|^2/3(\epsilon_F - \epsilon_a) > 0$, $J_a^{ST} = \sqrt{1 - \frac{1}{2}(\beta_l^2 + \beta_r^2)} J_a^T$ and $J_{lr} = -4V_l V_r \beta_l \beta_r / (\epsilon_F - \epsilon_f)$, so that $|J_{lr}|/J_a^T \approx \beta^2$. Both \mathbf{S} and \mathbf{M} vectors are involved in Kondo screening, a situation much richer than the one described by the single impurity Hamiltonian (5).

As far as the Kondo physics is concerned, the number of channels $n = 2$ exactly equals twice the spin, $2S$. Therefore, the physics in the strong coupling limit is similar to that of the *single* channel one. The two stable fixed points are $(J_a^T, J_a^{ST}, J_a^T, J_a^{ST}) = (\infty, \infty, 0, 0)$ implying $T_K = \max\{T_{Kl}, T_{Kr}\}$, $T_{Ka} = \{\exp[-1/(J_a^T + J_a^{ST})]\}$. In the weak coupling limit, systems with $2S > n$ and $2S = n$ might have different physics.

Finally, let us discuss the experimentally relevant situation of changing electron occupation N in the same TQD device. For $N = 2$, the lowest-energy states consist of two singlets $|S_a\rangle$ and two triplets $|T_a\rangle$ ($a = l, r$) (one electron in the left or right dot and one electron in the central dot). The next charged transfer excitons consist of a singlet $|S_{lr}\rangle$ and a triplet $|T_{lr}\rangle$ (one electron in the left and right dots). The corresponding energy levels are

$$\begin{aligned} E_{S_a} &= \varepsilon_f + \varepsilon_a - \frac{2W_a^2}{\Delta_a + Q_a} - \frac{W_a^2}{\Delta_a}, \\ E_{T_a} &= \varepsilon_f + \varepsilon_a - \frac{W_a^2}{\Delta_a}, \\ E_{S_{lr}} &= E_{T_{lr}} = \varepsilon_l + \varepsilon_r + W_l\beta_l + W_r\beta_r. \end{aligned} \quad (12)$$

where $\beta_a = W_a/\Delta_a \ll 1$, ($\Delta_a = \varepsilon_a - \varepsilon_f$).

The most symmetric case is realized when $\varepsilon_l = \varepsilon_r \equiv \varepsilon$ and $V_l = V_r \equiv V$. If at the end of the first stage RG procedure one has $E_{S_l} \simeq E_{T_l} \simeq E_{S_r} \simeq E_{T_r}$, the TQD possesses a $P \times SO(4) \times SO(4)$ symmetry (with P is $l \leftrightarrow r$ permutation). Following an RG procedure and a Schrieffer-Wolff transformation, the spin Hamiltonian reads,

$$\begin{aligned} H &= J_1^T \sum_a \mathbf{S}_a \cdot \mathbf{s}_a + J_1^{ST} \sum_a \mathbf{M}_a \cdot \mathbf{s}_a \\ &+ J_2^T \hat{P} \sum_a \mathbf{S}_a \cdot \mathbf{s}_{a\bar{a}} + J_2^{ST} \hat{P} \sum_a \mathbf{M}_a \cdot \mathbf{s}_{a\bar{a}} \\ &+ \sum_{a=l,r} [J_{lr}^T \mathbf{S}_a + J_{lr}^{ST} \mathbf{M}_a] \cdot (\mathbf{s}_{lr} + \mathbf{s}_{rl}), \end{aligned} \quad (13)$$

where $J_1^T(D_0) = J_2^T(D_0) = \frac{2(1-\beta^2)|V|^2}{\varepsilon_F - \varepsilon}$, $J_{lr}^T(D_0) = \frac{2\beta^2|V|^2}{\varepsilon_F - \varepsilon_f}$, and $J^{ST}(D_0) = \sqrt{1 - \frac{2W^2}{(\Delta+Q)^2}} J^T(D_0)$. Here again, the Kondo physics falls under the category $2S = n$. It is then sufficient to write (and solve) second order poor-man scaling equations. Having done it, we find the stable fixed points $J_i^T, J_i^{ST} \rightarrow \infty$ ($i = 1, 2$). These define the corresponding Kondo temperature

$$T_K = \exp\left(-\frac{2}{(\sqrt{3}+1)(J_1^T + J_1^{ST})}\right).$$

For $N = 4$, similar analysis shows that the TQD again manifests the fully screened Kondo resonance with the (∞, ∞) fixed point. Thus, varying the TQD occupation (by a gate voltage) through $N - 1$ even, N odd, $N + 1$

even, the corresponding system follows Fermi liquid, non Fermi liquid and again Fermi liquid behavior.

Summary: The novel achievements are: i) In composite quantum dots, such as the TQD in figure 1, a generic two-channel Kondo problem emerges, in which the impurity is a *real* spin, and the two-channel fermions are real electrons. The current is solely due to co-tunneling. This result is manifested in the spin Hamiltonian (5). ii) RG equations (6,7) for the exchange constants are solved (8) in the entire quadrant $J_{l,r} > 0$ and yield the flow diagram displayed in figure 2. iii) Inspecting the conductance $G(V_{ga}, T)$ as function of temperature (figure 3) and gate voltage (figure 4) suggest an experimentally detectable and controllable transition between one- and two-channel Kondo physics. iv) Analysis of the Kondo physics in cases of higher spin degeneracy of the dot ground state is carried out in relation with dynamical symmetries. The Kondo physics remains that of a Fermi liquid with $n = 2S$, and the corresponding Kondo temperatures are calculated. v) Electron occupation is intimately related to the nature of the Kondo physics ($n > 2S$ for $N = 3$ and $n = 2S$ for $N = 2, 4$). vi) One remark regarding non-linear response is in order. If a quantum dot in the two channel Kondo regime is subject to a *finite DC bias* there is a peculiar effect of oscillatory current response [12]. The TQD in series discussed here might then be used to test it experimentally.

Acknowledgment: We would like to thank A. Schiller for very helpful discussions. Support from BSF, ISF and DIP grants is highly appreciated.

-
- [1] P. Nozieres and A. Blandin, J. Phys. (Paris) **41**, 193 (1980).
 - [2] P. Schlottman and P.D. Sacramento, Adv. Phys. **42**, 641 (1993).
 - [3] D.L. Cox and A. Zawadowski, **47**, 599 (1999).
 - [4] K. A. Matveev, Phys. Rev. **B51**, 1743 (1995); Y. Oreg and D. Goldhaber-Gordon, cond-mat/0203302; E. Lebanon and A. Schiller, Phys. Rev. **B64**, 245338 (2001).
 - [5] L. Glazman and M. Raikh, JETP Lett. **47**, 452 (1988); T.-K. Ng and P. A. Lee, Phys. Rev. Lett., **61**, 1768 (1988).
 - [6] T. Kuzmenko, K. Kikoin, and Y. Avishai, Phys. Rev. Lett. **89**, 156602 (2002).
 - [7] F. D. M. Haldane Phys. Rev. Lett. **40**, 416 (1978).
 - [8] P. W. Anderson, J. Phys. C.: Solid. St. Phys., **3**, 2435 (1970).
 - [9] P. Coleman, *Local moment physics in heavy electron systems*, cond-mat/0206003.
 - [10] A. Kaminski, Yu. V. Nazarov, and L.I. Glazman, Phys. Rev. B **62**, 8154 (2000).
 - [11] I. Afleck and A. W. W. Ludwig, Phys. Rev. Lett. **67**, 3160 (1991).
 - [12] P. Coleman, C. Hooley, Y. Avishai, Y. Goldin and A. F. Ho, J. Phys. Condensed Matter **14** L205-L211 (2002).